INTERNATIONAL JOURNAL FOR NUMERICAL METHODS IN FLUIDS
Int. J. Numer. Meth. Fluids 2007; **53**:933–945
Published online 2 August 2006 in Wiley InterScience (www.interscience.wiley.com). DOI: 10.1002/fld.1313

Prediction of losses in the flow through the last stage of low-pressure steam turbine

Slawomir Dykas*,†, Włodzimierz Wróblewski‡ and Henryk Łukowicz§

Institute of Power Engineering and Turbomachinery, Silesian University of Technology, Konarskiego 18, PL 44100 Gliwice, Poland

SUMMARY

In this paper, the numerical modelling of the flow through the low-pressure steam turbine last stage was presented. On the basis of predicted wet steam flow-field, the aerodynamic as well as thermodynamic losses were estimated. For calculations of the wet steam steady flow-field three numerical methods were employed. The first method was a streamline curvature method (SCM). The commercial CFD code (CFX-TACflow) and an in-house code, both solving the 3-D RANS equations, were the next two methods. In the wet steam region, by means of all three methods, the equilibrium flow was modelled. Additionally, the in-house CFD code was used for modelling of the non-equilibrium steam condensing flow. In this work, the comparison of the cascade loss coefficient for stator and rotor and selected flow parameters for the stage were presented, compared and discussed. Copyright © 2006 John Wiley & Sons, Ltd.

Received 7 May 2006; Revised 21 June 2006; Accepted 23 June 2006

KEY WORDS: steam turbine; wet steam; condensation

INTRODUCTION

At present it is possible to predict the complicated 3-D viscous, turbulent and two-phase flow-field in turbomachinery by means of commercial as well as an in-house CFD codes solving RANS equations. To date, the aerodynamic and thermodynamic losses in steam turbine stages were investigated by many researchers. Both experimental researches (e.g. References [1–3]) and numerical ones [4, 5] are known in this field. The quality of aerodynamic losses estimation depends

*Correspondence to: Slawomir Dykas, Institute of Power Engineering and Turbomachinery, Silesian University of Technology, Konarskiego 18, PL 44100 Gliwice, Poland.
†E-mail: dykas@imiue.polsl.pl
‡E-mail: wroblews@imiue.polsl.pl
§E-mail: lukowicz@imiue.polsl.pl

on the discretization of the computational domain and employed numerical methods, like spatial discretization or turbulence model. In the case of wet steam flows, the correct calculations of steam parameters (thermal and calorical) and the two-phase flow model (equilibrium or non-equilibrium) are of great importance. Incorrect calculations of steam parameters affect the significant errors in thermodynamic and aerodynamic losses, because in these flows both types of losses do not occur separately.

In the methods based on the numerical solution to RANS equations in many cases, the flow-field and losses in steam turbines are calculated with the use of an ideal gas model. The application of ideal gas model for wet steam flow-field predictions is connected with errors by calculations of steam parameters and functions. Consequently, it results in incorrect values of the losses. Therefore, the application of the real gas model for wet steam flow modelling is undisputable.

The application of the real gas equation of state for solution to RANS equations creates many additional problems in the numerical algorithm. Therefore, many researchers decide to use the ideal gas model. For real gas model, the calculations become more time consuming, due to many implicit relations stemming from the non-linear form of gas equation of state. Even when the 'steam tables' are created before computation process, the search for the value in the table is more time consuming than using a simple explicit relation.

In the case of two-phase non-equilibrium wet steam flow there is a need to calculate the steam properties below the saturation line (for gas phase in metastable state). Usually, the real gas equation of state (virial or fundamental) is created for superheated and for metastable regions, and for high values of supercooling (outside its application range) this equation gives incorrect values. In order to avoid this problem, e.g. a new equation of state with the simple mathematical form represented by a low-order approximate surface of IAPWS-IF'97 standard can be used [6]. Due to the low order of approximate surface, determined for the fixed steam region, the steam properties can be smoothly extrapolated outside its boundaries. It is impossible in the case of IAPWS-IF'97 formulations, because the fundamental equation of state consists of the polynomials of the high order, which are very inaccurate outside the application range.

The next and very important issue in the flow modelling in turbomachinery, besides the access to blade geometry data, is to fix the boundary conditions at the stage inlet and outlet. The solution of this problem can be the experimental data or computation results using streamline curvature method (SCM) simulating the flow on the meridional plane [7].

Presented in the paper results were carried out for the last stage of outdated LP steam turbine with penultimate Baumann stage. For assumed load, the calculations by means of SCM for whole LP part were carried out. Obtained spanwise distributions of flow parameters in blade rows gaps were used as boundary conditions for 3-D RANS solvers.

NUMERICAL ANALYSIS

In the case of wet steam flows two types of losses have to be considered, namely aerodynamic losses and thermodynamic one (caused by formation and existence of the liquid phase), which interact in very complex way. The correct estimation of thermodynamic losses depends on an accurate determination of the steam parameters. Therefore, for modelling of these flows a real gas equation of state for steam has to be used. For all three methods, the real gas equations of state for steam and the equilibrium model below the saturation line were employed. Additionally, for in-house CFD code the non-equilibrium model with homogeneous and/or heterogeneous condensation was used.

Because of the lack of experimental data for the analysed stage, the SCM numerical results for whole LP part were applied as boundary conditions at the inlet and outlet of the stage for commercial and in-house CFD codes. The 3-D calculations with the use of commercial code and in-house CFD code were carried out for exactly the same numerical grid and the same turbulence model as a supplement to RANS equations. The differences were in the real gas equation of state and numerical methods.

Streamline curvature method (SCM)

The classical SCM was used to simulate the flow through the LP steam turbine stages on the meridional plane. In this method, the virial real gas equation of state for steam was applied [7].

In this method, the empirical formulas for energy dissipation into flow conservation equations were employed. The losses were divided into profile, boundary and additional ones, which include leakage and wetness losses. In this method, the empirical correlations proposed by Craig and Cox [8] were used, but for long blades (like for the last LP stages) the relations given by Aleksejeva [9] were implemented. The correlations including wetness losses were assumed according to Gyarmathy's work [10].

CFX-TASCflow commercial CFD code

Among available commercial CFD codes, the CFX-TASCflow is the most popular for turbomachinery applications. For the presented calculations the CFX-TASCflow v.2.11.1 [11] was used.

TASCflow is based on the averaged Navier–Stokes equations employing the finite volume method (FVM) with an implicit, multi-block algorithm. The solution strategy is based on the algebraic multi-grid method. TASCflow provides many types of turbulence models. However, for turbomachinery applications the Menter's SST (shear-stress-transport) turbulence model [12, 13] is recommended. In TASCflow, the real gas flow is modelled using the approximation of water steam tables. For wet steam region TASCflow has implemented two models, equilibrium dry/wet model and non-equilibrium dry/wet model (NES). In the presented calculations, the equilibrium model for two-phase flow was assumed, because by means of NES model the calculations were not successful, even with the help of CFX experts.

TraCoFlow in-house CFD code

The third method was the in-house ('academic') CFD code. The numerical simulation is based on the time-dependent 3-D RANS equations, which are coupled with a two-equation turbulence model (k–ω SST model), and additional mass conservation equations for the liquid phase (two for homogeneous and one for heterogeneous condensation). The set of 10th governing equations is closed by a 'local' real gas equation of state [6]. The idea of used real gas equation of state consists in the creation of an equation of state with as simple mathematical form as possible, but simultaneously very accurate. Because the flow through turbine stages takes place in a limited range of steam parameters, the equation of state covering the whole region of superheated steam is unnecessary. The simple mathematical form can be very accurate, but only in the small parameters range. For these reasons the new form of the equation of state for real gases was created (Figure 1).

DOI: 10.1002/fld

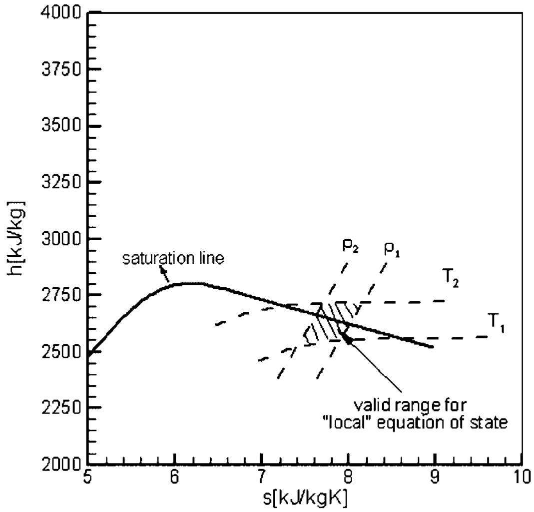

Figure 1. Mollier diagram of the 'local' real gas equation of state near the saturation line.

The mathematical form of used real gas equation of state (1) is similar to the virial equation of state with one virial coefficient.

$$\frac{v \cdot p}{R \cdot T} = z(T, v) = A(T) + \frac{B(T)}{v} \tag{1}$$

where

$$A(T) = a_0 + a_1 \cdot T + a_2 \cdot T^2$$

$$B(T) = b_0 + b_1 \cdot T + b_2 \cdot T^2$$

The coefficients a_i, b_i $(i = 0, 1, 2)$ of the polynomials $A(T)$ and $B(T)$ are the functions of temperature only, and can be found from an approximation of thermodynamic properties of steam IAPWS-IF'97 [14]. It is easy to notice, that this equation is represented by a relatively uncomplicated approximate surface (Figure 2).

The equation of state (1) is called the 'local' real gas equation of state, because due to the simple mathematical form it can be applied locally in a limited parameter range only.

Expressions for enthalpy, entropy and other properties can be determined from the following thermodynamic relations [6]:

$$\begin{aligned} h &= h_{\text{ref}} + \Delta h \\ s &= s_{\text{ref}} + \Delta s \\ c_p &= c_{p_{\text{ref}}} + \Delta c_p \\ c_v &= c_{v_{\text{ref}}} + \Delta c_v \end{aligned} \tag{2}$$

DOI: 10.1002/fld

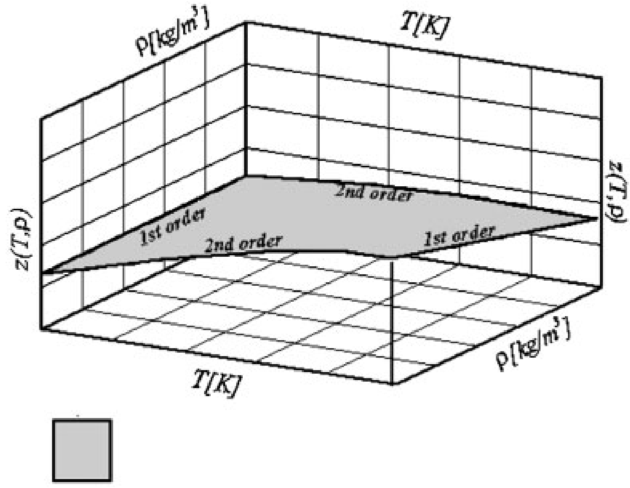

Figure 2. Approximate surface of the IAPWS-IF97 properties.

where h_{ref}, s_{ref}, etc. are the referential parameters. The real gas corrections are defined as follows:

$$
\begin{aligned}
\Delta h &= R\cdot T\int_0^\rho \left(\frac{\partial z}{\partial T}\right)_\rho \frac{\mathrm{d}\rho}{\rho} + R\cdot T\cdot(1-z)\\
\Delta s &= R\int_0^\rho \left(\frac{z_T-1}{\rho}\right)\mathrm{d}\rho + R\cdot \ln(\rho\cdot R\cdot T)\\
\Delta c_v &= R\cdot T\int_0^\rho \left(\frac{\partial z_T}{\partial T}\right)_\rho \frac{\mathrm{d}\rho}{\rho}\\
c_p - c_v &= R\frac{z_T^2}{z_v}
\end{aligned}
\tag{3}
$$

On the basis of gas equation of state (1) the derivatives of the compressibility coefficient are calculated from:

$$
z_T(T,v) = z + T\cdot\left(\frac{\partial z}{\partial T}\right)_v \quad \text{and} \quad z_v(T,v) = z - v\cdot\left(\frac{\partial z}{\partial v}\right)_T \tag{4}
$$

In addition, the speed of sound and the isentropic exponent are determined in the same way:

$$
\begin{aligned}
a^2 &= R\cdot T\cdot\left(\frac{R}{c_v}\cdot z_T^2 + z_v\right)\\
\gamma &= \frac{1}{z}\cdot\left(\frac{R}{c_v}\cdot z_T^2 + z_v\right)
\end{aligned}
\tag{5}
$$

The conception of the 'local' real gas equation of state can be applied to determine the thermodynamic properties of the any arbitrary real gas, in each case when the simply mathematical form is needed.

For the two-phase non-equilibrium flow it was assumed that the volume occupied by droplets is negligibly small. The droplets formed by homogeneous nucleation are very small and can grow. The interaction between the droplets is not taken into account in the model. The heat exchange between the liquid phase and the solid boundary, and the velocity slip between vapour and the liquid phase are neglected. The non-slip assumption is much less significant than the effects of the thermal non-equilibrium [15]. The conservation equations are formulated for the two-phase mixture with the specific parameters calculated from the following relations:

$$\begin{aligned} h &= h_g(1-y) + h_1 y \\ s &= s_g(1-y) + s_1 y \\ \rho &= \rho_g/(1-y) \end{aligned} \tag{6}$$

The value of the non-equilibrium wetness fraction y is calculated from the conservation equations for the liquid phase.

The condensation phenomena were modelled on the ground of the classical nucleation theory of Volmer, Frenkel and Zeldovich, which is well suited for modelling of technical flows [16, 17]. The nucleation rate was calculated with the correction factor proposed by Kantrowitz [18]. The equation of droplet growth for steam flow requires relation valid for the wide range of Knudsen numbers. Therefore, in the presented method the continuous model proposed by Gyarmathy [19] was used.

For heterogeneous condensation, an additional governing equation has to be solved. The model of heterogeneous condensation is based on the work of Gorbunov and Hamilton [19].

The system of governing equations was solved on a multi-block structured grid with the use the FVM and integrated in time with the explicit Runge–Kutta method. For integration in time, the fractional step method was used to split the equations into a homogeneous and an inhomogeneous part in order to introduce different time steps for the flow and condensation calculations.

The MUSCL technique is implemented to approach the TVD scheme with the flux limiter to avoid oscillations. A detailed description of the numerical method can be found in References [6, 20].

Loss coefficient

Many forms of loss coefficients for the flow through the turbine stages are known. The basic correlation uses the entropy increase. This relation is known as the cascade (entropy or Markov) loss coefficient:

$$\zeta = \frac{T_2 \Delta s}{\frac{1}{2} w_{2s}^2} \tag{7}$$

In Equation (7), in the case of the flow through the rotor the relative velocities were used. As for the stator, the absolute velocities have to be assumed. For 3-D test cases, this coefficient is calculated along the blade length using the circumferentially mass averaged values. Many other forms of loss coefficients include the relation stemming from ideal gas model, therefore they were not used in the presented analysis.

CALCULATION RESULTS

A numerical analysis was carried out for the geometry of the last stage of outdated 200 MW LP steam turbine (Figure 3). The assumed operating conditions ($p_0 = 10\,\text{kPa}$, $T_0 = 320.5\,\text{K}$ and $p_2 = 2.7\,\text{kPa}$) corresponding to the power of 140 MW were chosen, because for these conditions the condensation starts in the last stage only.

The boundary conditions at the inlet and outlet for TASCflow and TraCoFlow CFD code were determined using SCM calculations for whole LP part. The numerical results represent the steady flow-field. It means that the presented losses and flow parameters are time averaged. For modelling the stator–rotor interaction a mixed-out technique [21] was used. The tip leakage was not taken into account, because rotor tip clearance was not modelled.

For TASCflow and TraCoFlow CFD codes exactly the same numerical grid was applied. The computational domains for RANS calculations were discretized by means of the structural multi-block grid (Figure 4). The dimensionless distance of the first grid line from solid walls, y^+, was less than 1.5. Numerical grids for the last stator and rotor consisted of about 260 000 nodes. The Reynolds number calculated with the use of the total parameters at the inlet, the inlet speed of sound and blade chord was $Re = 0.17 \times 10^6$. Our former research showed that for RANS model the number of grid points close to 250 000 for one blade row makes the solution grid independent. A further increase in the grid points does not change the flow-field significantly and does not change the values of the loss coefficient (for steady flow and without tip leakage).

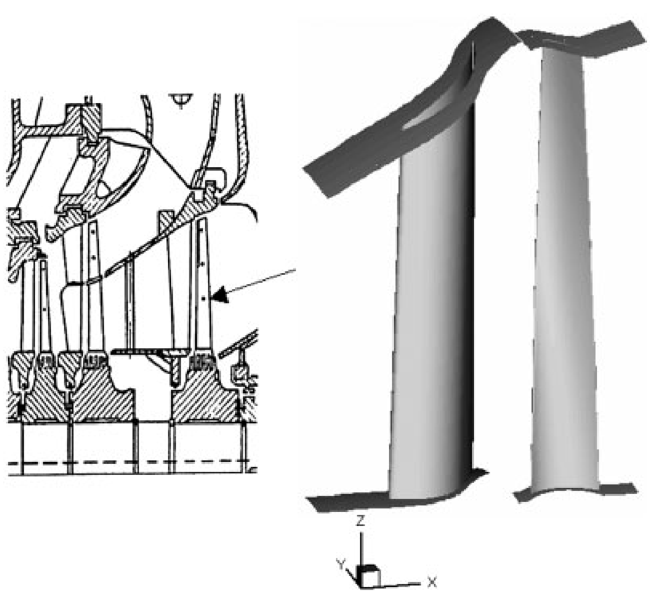

Figure 3. Geometry for the LP steam turbine last stage.

DOI: 10.1002/fld

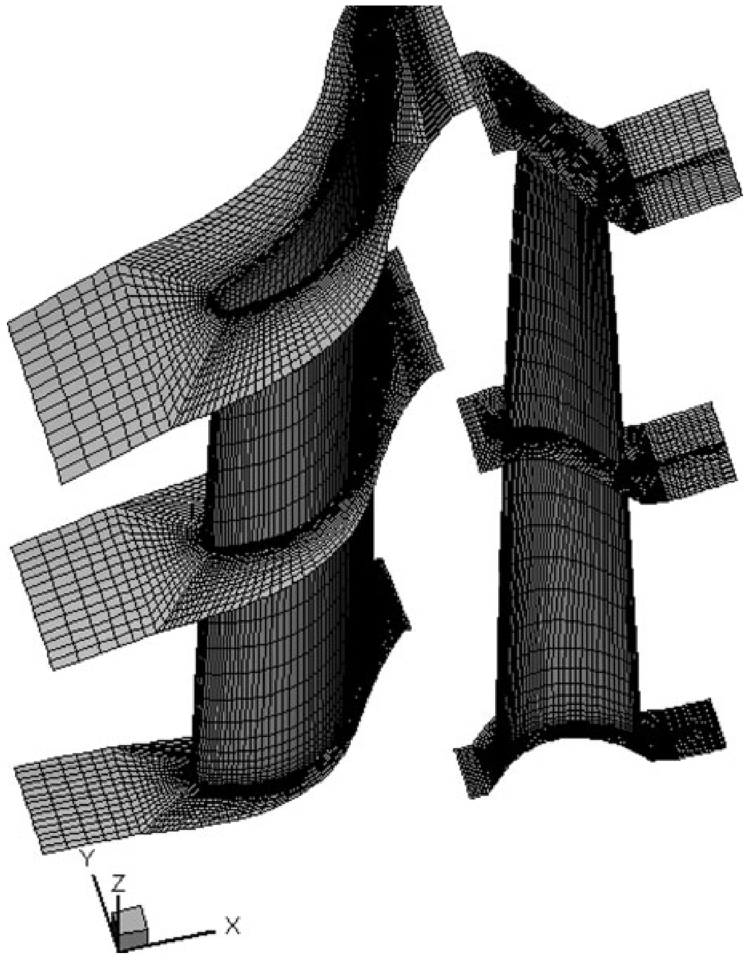

Figure 4. Numerical grid used for the last stage.

The spanwise distributions of parameters were calculated with the use of circumferentially mass averaged quantities at the inlet, in stator–rotor gap and at the stage outlet. The distributions of loss coefficients were determined taking into account the spanwise distributions of the mass flow rate, which allowed to calculate the loss coefficients approximately on the streamlines.

The five sets of results obtained by means of three methods were discussed. The results for equilibrium flow model (SCM, TASCflow and TraCoFLow codes) and for two non-equilibrium flow models (TraCoFlow code with homogeneous condensation and with heterogeneous condensation on insoluble particles with concentration 10^{14} particles per kilogram and with the radius 10^{-8} m) were considered. For assumed concentration of solid impurities, the heterogeneous condensation was dominated in the flow.

The spanwise distributions of loss coefficients for the stator and rotor were presented in Figure 5. The loss coefficients obtained by means of SCM, TASCflow and TraCoFlow codes with equilibrium

DOI: 10.1002/fld

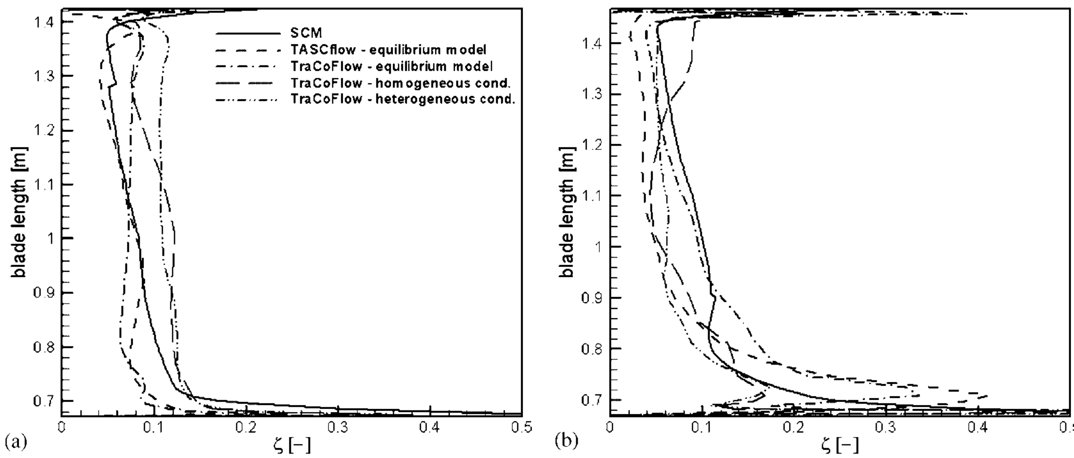

Figure 5. (a) Spanwise distributions of the loss coefficients for the last stage stator; and (b) rotor.

wet steam model were compared with the losses calculated using TraCoFlow code with non-equilibrium models. For stator (Figure 5(a)) the values of the losses for equilibrium model are similar, whereas the losses calculated using non-equilibrium flow-field are higher along the whole blade length. Usually, the condensation process is connected with higher entropy increase. The losses distributions in the rotor (Figure 5(b)) have more complicated character. The significant increase in the losses close to the hub was observed. It follows from the fact that close to the hub the flow through the rotor is chocked. For TASCflow numerical results this increase is the biggest, what corresponds to the very high expansion in stator close to the hub.

Besides the loss coefficient, very interesting for the stage work is to present the spanwise distributions of the degree of reaction and static enthalpy drop (Figures 6(a) and (b)). Degree of reaction was calculated by means of the real enthalpy drops in rotor and stage. Close to the hub the negative values of reaction were observed (Figure 6(a)), what means that the compression in rotor takes place. For all results the values of enthalpy drop in stage are very similar (Figure 6(b)). Calculated mass flow rate was presented in Table I. The maximum difference between calculated mass flow rates was about 0.5%.

The distributions of an absolute angle and absolute velocity at the stage outlet were presented in Figure 7. For the last stage, the outlet velocity represents the outlet losses. For SCM and TASCflow results the clear decrease in the outlet velocity close to the hub was visible (Figure 7(b)). For TASCflow results, this region was even 0.2 meter high. In the case of TraCoFlow results, this decrease was not so significant. The absolute outlet angle for all cases was in the range between 80° and 100° (Figure 7(a)). The distributions of absolute outlet angle for TASCflow and TraCoFlow non-equilibrium model are very similar.

The spanwise distributions of the wetness fractions in the stator–rotor gap and at the stage outlet were presented in Figures 8(a) and (b). For the non-equilibrium flow models, the wetness was lower than in the case of equilibrium model in stator and rotor. For non-equilibrium calculations the maximum outlet droplet radii were about 0.07 μm, and was located at 70% blade span.

Figure 9 shows the comparison between TraCoFlow and TASCflow code results for the static pressure and specific entropy distributions on the stator and rotor blades close to the hub. The

DOI: 10.1002/fld

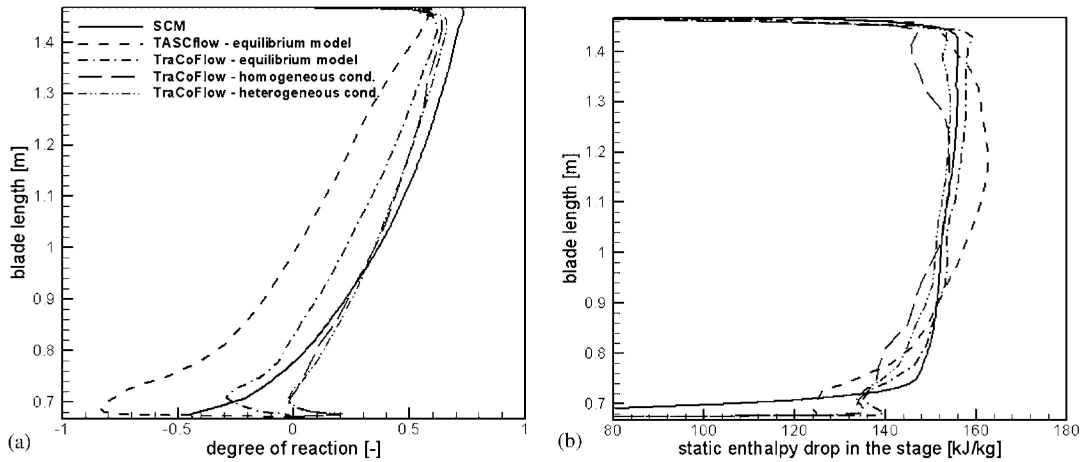

Figure 6. (a) Spanwise distributions of the degree of reaction; and (b) specific enthalpy drop for the stage.

Table I. Values of mass flow rate.

	SCM	TASCflow	TraCoFlow equilibrium	TraCoFlow homogeneous condensation	TraCoFlow heterogeneous condensation
Mass flow rate (kg/s)	23.32	23.34	23.38	23.41	23.40

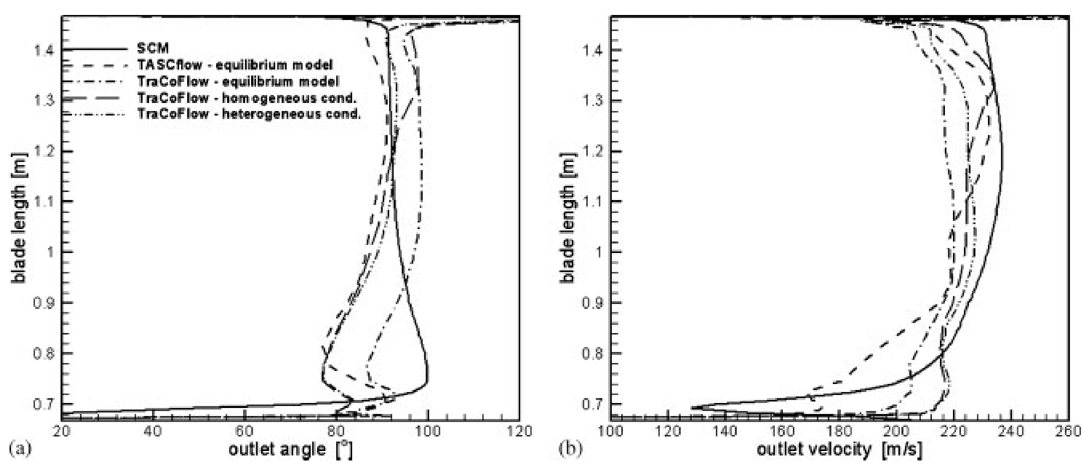

Figure 7. (a) Spanwise distributions of the absolute outlet angle; and (b) velocity at the stage outlet.

visible differences follow probably from the assumed real gas equation of state for steam. In the case of TASCflow results, the very low pressure ($\sim$ 600 Pa) was observed on the stator blade close to the trailing edge. A very high entropy increase corresponds to this value of pressure, which seems to be unrealistic for steam. In addition, for TASCflow results too high entropy increase is observed in the rotor in comparison with the stator.

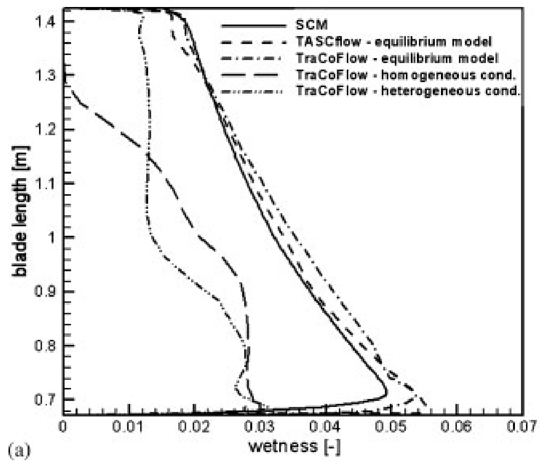

Figure 8. (a) Spanwise distributions of the wetness fraction at the rotor inlet; and (b) rotor outlet.

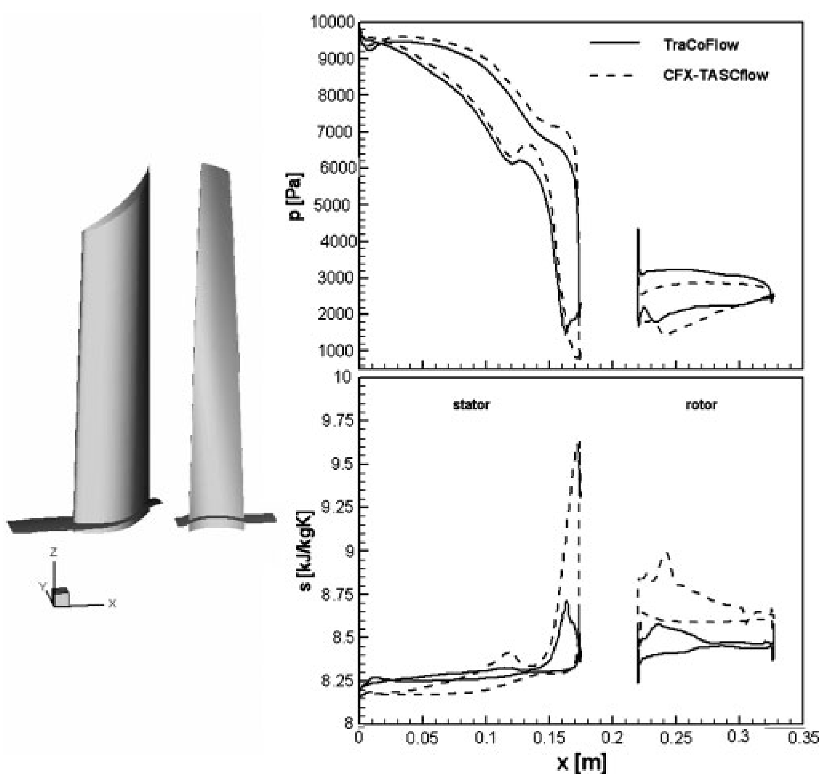

Figure 9. Static pressure and specific entropy distributions on the stator and rotor blade profiles close to the hub.

DOI: 10.1002/fld

CONCLUSIONS

Three numerical methods were used to predict the wet steam flow-field and to estimate the losses in the last stage of LP steam turbine. The results for equilibrium wet steam flow obtained by means of the finite volume methods (FVM), namely TASCflow and TraCoFlow codes were compared with the streamline curvature method including the empirical correlations for the loss coefficients. In addition, with the use of in-house CFD code the results for non-equilibrium steam condensing flow were presented.

From the carried out numerical analysis the differences between used methods were observed. For equilibrium model, the differences between TASCflow and TraCoFlow results follow probably from the accuracy in calculation of the steam properties below the saturation line. Significant differences were visible for the steam parameters, like entropy and enthalpy.

The presented distributions of loss coefficients have qualitatively similar characters and values. If the experimental data for the analysed stage were accessible, a more detailed comparison would not be possible, because the measurements in real LP steam turbine are very difficult and inaccurate, and it is impossible to measure in stator–rotor gaps.

The Streamline Curvature Method turned out to be a very convenient tool for the estimations of the boundary conditions for further detailed 3-D RANS computations. The presented academic CFD code has the quality comparable to commercial code, and the application of the 'local' real gas equation of state assure the correct estimation of the steam parameters.

Lately, the rapid increase in the use of commercial CFD codes by university researchers was observed. However, the presented results show that the further research on development of so-called 'academic' CFD codes is needed, and the commercial CFD code results have to be treated cautiously and need careful analysis as well.

NOMENCLATURE

a	speed of sound (m/s)
c_p, c_v	specific heats (J/(kg K))
h	specific enthalpy (J/kg)
p	pressure (Pa)
R	individual gas constant (J/(kg K))
s	specific entropy (J/(kg K))
T	temperature (K)
w	velocity (m/s)
y	wetness fraction (kg/kg)
z	compressibility coefficient
ρ	density (kg/m^3)
γ	adiabatic exponent
v	specific volume (m^3/kg)
ζ	cascade loss coefficient
Δ	quantity increase

Subscripts

0	total parameter
1	inlet

DOI: 10.1002/fld

2	outlet
g	vapour phase
l	liquid phase
s	isentropic quantity

Abbreviations

LP	low-pressure
RANS	Reynolds averaged Navier–Stokes
SCM	streamline curvature method

REFERENCES

1. Bohn D, Holzenthal K. Measurement of the wetness fraction and droplet size distribution in a condensation turbine. *Proceedings of the 2nd European Conference on Turbomachinery*, Antwerpen, Belgium, 1997; 55–63.
2. Dibelius GH, Mertens K, Pitt RU, Strauf E. Investigation of wet steam flow in turbines. *Proceedings of the Institute of Mechanical Engineers*, *Conference on Turbomachinery-Efficiency*, *Prediction and Improvement*, Cambridge, U.K., 1987; 135–143.
3. Vomela J. Experimental research of turbine stages. *Power Machines 2002*, *Conference*, WBU in Pilsen, 2002.
4. Bohn D, Surken N, Kreitmeier F. Nucleation phenomena in a multi-stage low pressure steam turbine. *Proceedings of the 5th European Conference on Turbomachinery*, Prague, 2003.
5. Lampart P. Numerical optimization of 3D blading in the LP exit stage of steam turbine for different load conditions. *5th European Conference on Turbomachinery*, Prague, 2003.
6. Dykas S. Numerical calculation of the steam condensing flow, task quarterly. *Scientific Bulletin of Academic Computer Centre in Gdansk* 2001; **5**(4):519–535.
7. Chmielniak T, Łukowicz H. Flow investigations for different loads of blade cascade. *ZN Politechniki Śląskiej*, *z.*, vol. 126, Gliwice, 1995 (in Polish).
8. Craig HRM, Cox HJA. Performance estimation of axial flow turbines. *Journal of the Institute of Mechanical Engineers* 1970–71; **32**:407–424.
9. Aleksejeva RN, Bojcova EA. Approximate method of calculation of the energy losses in the blade cascade. *Teploenergetika* 1973; **12**:21–25 (in Russian).
10. Gyarmathy G. Grunglagen einer Theorie der Nassdampfturbine. *Dissertation*. Juris Verlag, Zürich, 1960.
11. CFX-TASCflow, theory documentation. *Version 2.11*, AEA Technology, Canada, 2001.
12. Menter FR. Two-equation eddy-viscosity turbulence models for engineering applications. *AIAA Journal* 1994; **32**:1598–1605.
13. Menter FR. A comparison of some recent eddy-viscosity turbulence models. *Journal of Fluids Engineering* 1996; **118**:514–519.
14. Wagner W *et al*. The IAPWS industrial formulation 1997 for the thermodynamic properties of water and steam. *Transactions of the ASME*, *Journal of Engineering Gas Turbines and Power* 2000; **122**:150–182.
15. White AJ, Young JB, Walters PT. Experimental validation of condensing flow theory for a stationary cascade of steam turbine blades. *Philosophical Transactions of the Royal Society of London*, *Series A* 1996; 354–359.
16. Frenkel J. *Kinetic Theory of Liquids*. Dover Publishers: New York, 1955.
17. Fuchs NA, Satugin AG. *High-Dispersed Aerosols*, *Topics in Current Aerosols Research*, Hidy GM, Brock JR (eds). Pergamon Press: London, 1971.
18. Kantrowitz A. Nucleation in very rapid vapour expansions. *Journal of Chemical Physics* 1951; **19**:1097–1100.
19. Gorbunov B, Hamilton R. Water nucleation on aerosol particles containing both soluble and insoluble substances. *Journal of Aerosol Science* 1997; **28**(2):239–248.
20. Wróblewski W. Numerical simulation of the flow phenomena in thermal turbines. *ZN Politechniki Śląskiej*, *s. Energetyka* 2000; **132** (in Polish).
21. Giles MB. UNSFLOW: a numerical method for the calculation of unsteady flow in turbomachinery. *GTL Report No. 205*, 1991.

DOI: 10.1002/fld